Available online at www.sciencedirect.com
ScienceDirect
Journal of Sound and Vibration 315 (2008) 414–432
JOURNAL OF SOUND AND VIBRATION
www.elsevier.com/locate/jsvi

Second-order solutions for the dynamics of a semi-infinite cable on a unilateral substrate

Lucio Demeio[a,*], Stefano Lenci[b]

[a]*Dipartimento di Scienze Matematiche, Università Politecnica delle Marche, Via Brecce Bianche 1, I-60131 Ancona, Italy*
[b]*Dip. di Architettura, Costruzioni e Strutture, Università Politecnica delle Marche, Via Brecce Bianche 1, I-60131 Ancona, Italy*

Accepted 5 March 2008
The peer review of this article was organised by the Guest Editor
Available online 21 April 2008

Abstract

We present an asymptotic solution of a moving-boundary problem which describes the nonlinear oscillations of semi-infinite cables resting on an elastic substrate reacting in compression only, and subjected to a constant distributed load and to a small harmonic displacement applied to the finite boundary. Our solution is correct through the second-order terms in a smallness parameter, which we identify with the amplitude of the harmonic oscillation at the boundary, and it complements the first-order solution presented in an earlier work. The second-order analysis confirms the existence of two different regimes in the behaviour of the system, one below (called subcritical) and one above (called supercritical) a certain critical (cutoff) excitation frequency. In the latter, energy is lost by radiation at infinity, while in the former this phenomenon does not occur and various resonances are observed instead. We show that these two regimes exist at all orders in the expansion parameter, and that the cutoff frequency decreases at each order. We also perform a limited comparison of our asymptotic results with a numerical solution. The two approaches show very good agreement.

1. Introduction

In this work, we continue our investigations [1–3] of a moving-boundary problem for the wave equation, which arises, e.g., in the modeling of the J-lay technique [1] for marine pipelines or cables, or in marine moorings [4]. The mechanical system under consideration consists of a semi-infinite cable resting on a (unilateral) elastic substrate reacting in compression only, subjected to a constant distributed load and to a harmonic displacement applied to the finite boundary, which induces nonlinear forced oscillations. With regard to the J-lay problem, this model describes only the laid part and the first part of the suspended span, which are divided by the so-called Touch-Down Point (TDP) (Fig. 1). Since the position of the TDP is an additional unknown, which depends upon the solution itself, the resulting dynamics is governed by a nonlinear moving-boundary problem [5].

*Corresponding author.
E-mail addresses: demeio@mta01.univpm.it (L. Demeio), lenci@univpm.it (S. Lenci).
URL: http://www.dipmat.univpm.it/~demeio (L. Demeio).

0022-460X/$ - see front matter © 2008 Elsevier Ltd. All rights reserved.
doi:10.1016/j.jsv.2008.03.010

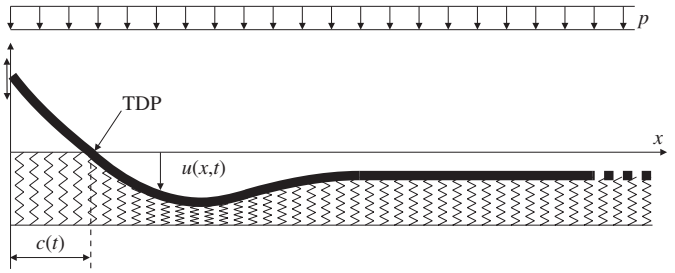

Fig. 1. A schematic picture of the considered mechanical systems.

The statics of continuous systems (cables, beams, plates), both of finite [6] and infinite [7] length and subjected to unilateral constraints, has been deeply investigated, both analytically [8] and numerically [9]. Also the dynamics of various continuous structures with bilateral nonlinear terms has been investigated in the past, both for finite [10] and infinite [11] domains, especially in the case of moving loads [12].

On the contrary, much less attention has been paid to the *dynamics* of continuous systems with *unilateral* distributed constraints, in particular to the case of cables on unilateral substrates, which is considered in this work. Analytical solutions for the motion of finite length beams on unilateral elastic springs have been obtained by Weitsman [13], while numerical solutions of the same problem have been obtained by Celep et al. [14]. The response of a finite beam on a tensionless Pasternak foundation subjected to a harmonic load was studied by Cokşun [15], who also considered the case of Winkler nonlinear soil [16]. The free and forced dynamics of a finite beam on a rigid and curved unilateral constraint has been investigated in Ref. [17]. Toscano [18] obtained some theoretical results but did not provide analytical solutions for the governing equations.

In Ref. [3] analytical and numerical solutions for a semi-infinite beam on a unilateral Winkler soil have been obtained and compared with each other. A steadily moving load acting on an infinite beam on a unilateral Winkler soil, a problem for railtracks, has been investigated by Choros and Adams [19]. Still in the framework of railway engineering, Metrikine [20] studied the pantograph–power line dynamical interaction by considering an infinite cable on a unilateral nonlinear soil under moving loads. He obtained a very elegant analytical solution; the substrate is modeled as an elastic half-space by Adams [21]. In Ref. [2] analytical solutions were obtained by the asymptotic method for semi-infinite cables and beams with unilateral elastic springs.

Although in the statical regime exact solutions can be found, even for large displacements (see, e.g., Ref. [22]), in the dynamical regime an exact, analytical solution of the nonlinear model equations is unattainable even for small displacements; therefore, we resort to an approximate solution by using asymptotic analysis [23,24]. The first-order solution was presented in Ref. [2], and in this paper we present the second-order solution, which is necessary to achieve better understanding of the nonlinear dynamics. In fact, the second-order terms are the first ones which are influenced by the nonlinearities of the problem.

In our perturbation expansion, the zero-order terms correspond to the static solution obtained in the absence of a time-dependent excitation applied at the boundary. The first-order terms permit to understand the primary resonance behaviour and the questions related to the wave propagation towards infinity [25,26]. In particular, these terms permit to identify two different regimes, below and above a certain critical (cutoff) excitation frequency, with very different wave properties [25]. These two regimes are present at all orders of the perturbative solution; here we analyse in detail the second-order behaviour, and infer from it the behaviour at higher-order terms. In particular, we show how the higher-order cutoff frequencies are related to the first-order one, a result which is not detectable by the first-order analysis.

From our asymptotic solution, we obtain the behaviour of the vertical displacement profiles as function of time and of the amplification factor D, which will be defined in Section 3.1 as the ratio between the amplitude of the oscillations of the TDP and the amplitude of the forcing oscillation imposed at the finite boundary. We use this synthetic parameter to show the main characteristics of the solution behaviour at various orders. In particular, from the dependence of D from the external frequency ω we detect all primary and secondary

resonances. The presence of the secondary resonances and their relationships with the primary resonances are both due to the nonlinearity, and can be detected only by the second-order analysis.

This paper is organized as follows: in Section 2 we introduce the mathematical model; in Section 3 the perturbative expansion solution is obtained. In Section 4 we report the second-order solution of the governing equations, which are the main results of this paper; in Section 5 we present some comparisons with numerical results, and in Section 6 we state our conclusions.

2. The mathematical model and changes of coordinates

The profile of the cable is represented by the function $u(x,t)$, where $0 \leqslant x < +\infty$ is the space variable and $t \geqslant 0$ the time. A constant downward load acts on the whole cable, while a restoring elastic force is present only on the portion of the spatial domain where the solution $u(x,t)$ is negative. This describes the action of the elastic substrate that acts in compression only (e.g., a Winkler soil), and represents the unique source of nonlinearity in the model (Fig. 1).

We assume that there exists only one point of the domain, $x = c(t)$, called Touch-Down Point, where the profile function vanishes, namely $u(c(t),t) = 0$; in particular, we suppose that $u(x,t) > 0$ for $0 \leqslant x < c(t)$ and $u(x,t) < 0$ for $c(t) < x < \infty$. This hypothesis is supported by the following consideration. When only a positive static displacement is applied at the finite boundary, the static configuration clearly has only one TDP [2] and, if the superimposed dynamic excitation is small enough, as assumed in this work, the TDP remains unique.

The static solution $u(x,t) \equiv u_S(x)$ plays an important role. In this case, $c(t) \equiv c_0$ is a constant. In this work, we shall look for time-dependent solutions of the boundary-value problem that correspond to small oscillations around the static solution. These oscillations are induced by a harmonic displacement applied at the $x = 0$ boundary. The TDP $x = c(t)$ then exhibits an oscillating behaviour as well, which we describe in short by means of its ratio with the oscillation amplitude of the boundary (see Section 3.1).

The dimensionless governing equations are given by [2]

$$\frac{\partial^2 u}{\partial t^2} - \frac{\partial^2 u}{\partial x^2} + 1 = 0, \quad 0 < x < c(t), \tag{1}$$

$$\frac{\partial^2 u}{\partial t^2} - \frac{\partial^2 u}{\partial x^2} + u + 1 = 0, \quad x > c(t). \tag{2}$$

Here, x (the space variable) is measured in terms of $v\sqrt{\rho/\gamma}$, t (the time variable) is measured in units of $\sqrt{\rho/\gamma}$ and u (the cable vertical displacement, positive in the upper direction) in units of p/γ, where γ is the elastic constant of the springs, $v = \sqrt{T/\rho}$ the propagation speed, T the constant traction in the cable, ρ the mass linear density and p is the uniformly distributed static load, which represents, for example, the cable self-weight.

In fact, the dimensionless x variable defined in Ref. [2] differs by a factor $\sqrt{2}$ with respect to the one introduced here, which brings in an extra factor in some of the terms of the equations. This factor is however inessential. The constant term $+1$ represents the external constant load applied to the system.

The boundary condition at $x = 0$ is

$$u(0,t) = U_0[1 + \varepsilon \sin(\omega t)], \tag{3}$$

while we require that $u(x,t)$ be bounded as $x \to \infty$; moreover, we assume that, whenever the equations support sustained traveling-wave solutions, terms corresponding to waves returning from $+\infty$ are not present, so that only "outgoing" waves (traveling to the right) are admitted [25,26]. Finally, the additional continuity conditions at $x = c$ are

$$u(c^-,t) = u(c^+,t) = 0, \tag{4}$$

$$\frac{\partial u}{\partial x}(c^-,t) = \frac{\partial u}{\partial x}(c^+,t), \tag{5}$$

where $c = c_0$ for static solutions and $c = c(t)$ for time-dependent solutions.

The static solution, $u_S(x)$, is obtained by switching off the time derivatives in Eqs. (1) and (2) and setting $\varepsilon = 0$ in the boundary condition (3). We will discuss it in the next section; here, we only anticipate the expression for the static TDP c_0, which is an important parameter in our analysis and is given by [2]

$$c_0 = \sqrt{1 + 2U_0} - 1. \tag{6}$$

This expression shows that there is a one-to-one correspondence between c_0 and U_0; for this reason, we will use either c_0 or U_0, whichever is more convenient, as a governing parameter in our analysis. The other one is the excitation frequency ω.

It proves convenient to introduce a variable transformation from the original variables (x, t) to a new set of variables (z, τ), in which the problem becomes either a fixed-boundary problem or a moving-boundary problem with the moving boundary at the finite end of the whole domain ($x = 0$ in the original formulation). A possible transformation which leads to a fixed-boundary problem is given by

$$z = \frac{x}{c(t)}, \quad \tau = t, \tag{7}$$

which was adopted in Ref. [2], where the first-order solution was obtained. The same transformation, however, was not suited for the second-order analysis, since the second-order terms presented secular behaviour in space for $z \to \infty$, which was not easy to eliminate by using well-established techniques [23,24].

In the present work, we adopt a different variable transformation,

$$z = x - c(t), \quad \tau = t, \tag{8}$$

with $u(x, t) = u(z + c(t), t) = U(z, t)$, which leads to a moving-boundary problem with the moving boundary at the finite end of the domain. In the following, in order to simplify the notation, we will use $u(z, t)$ instead of $U(z, t)$ for the new unknown function. With this transformation, the moving TDP $x = c(t)$ becomes $z = 0$ and is now fixed, so that $u(0, t) = 0$, while $x = 0$ and $x \to \infty$ correspond to $z = -c(t)$ and $z \to \infty$, respectively. As we shall see, the first-order solution obtained with this variable transformation agrees with the solution obtained in Ref. [2] and, in addition, no secular terms appear at the second order.

After evaluating all composed derivatives by using the chain rule, we obtain the transformed differential equations for the new unknown function $u(z, t)$:

$$\frac{\partial^2 u}{\partial t^2} + \left[\left(\frac{\mathrm{d}c}{\mathrm{d}t}\right)^2 - 1\right]\frac{\partial^2 u}{\partial z^2} - 2\frac{\mathrm{d}c}{\mathrm{d}t}\frac{\partial^2 u}{\partial t\,\partial z} - \frac{\mathrm{d}^2 c}{\mathrm{d}t^2}\frac{\partial u}{\partial z} + 1 = 0, \quad -c(t) < z < 0, \tag{9}$$

$$\frac{\partial^2 u}{\partial t^2} + \left[\left(\frac{\mathrm{d}c}{\mathrm{d}t}\right)^2 - 1\right]\frac{\partial^2 u}{\partial z^2} - 2\frac{\mathrm{d}c}{\mathrm{d}t}\frac{\partial^2 u}{\partial t\,\partial z} - \frac{\mathrm{d}^2 c}{\mathrm{d}t^2}\frac{\partial u}{\partial z} + u + 1 = 0, \quad z > 0, \tag{10}$$

with the boundary conditions

$$u(-c(t), t) = U_0[1 + \varepsilon \sin(\omega t)], \tag{11}$$

$$u(z, t) \quad \text{bounded as } z \to \infty, \tag{12}$$

and the additional continuity conditions

$$u(0^-, t) = u(0^+, t) = 0, \tag{13}$$

$$\frac{\partial u}{\partial z}(0^-, t) = \frac{\partial u}{\partial z}(0^+, t). \tag{14}$$

3. Perturbative approach

The moving-boundary conditions at the TDP make the problem very hard to approach. However, since we are interested in motions corresponding to small deviations from the static solution, we approach the problem

by using a perturbative expansion [23]

$$u(z,t) = u_0(z) + \varepsilon u_1(z,t) + \varepsilon^2 u_2(z,t) + \mathcal{O}(\varepsilon^3), \tag{15}$$

$$c(t) = c_0 + \varepsilon c_1(t) + \varepsilon^2 c_2(t) + \mathcal{O}(\varepsilon^3). \tag{16}$$

Note that, according to Eq. (11), the zero-order terms are independent of time and therefore, with this expansion, the zero-order quantities will be given by the static solution, consistently with our search for motions near the static profiles. Since we shall look for solutions that correspond to periodic oscillations, we shall assume that the functions $u_k(z,t)$ and $c_k(t)$, $k \geqslant 1$, admit a Fourier expansion of the type

$$u_k(z,t) = g_{k0}(z) + \sum_{n=1}^{\infty} [f_{kn}(z)\sin(n\omega t) + g_{kn}(z)\cos(n\omega t)], \tag{17}$$

$$c_k(t) = b_{k0} + \sum_{n=1}^{\infty} [a_{kn}\sin(n\omega t) + b_{kn}\cos(n\omega t)]. \tag{18}$$

Our aim is to determine the coefficients f, g, a, and b of these expansions.

We introduce the perturbative expansion (15) and (16) into the transformed equations (9) and (10) and obtain the following hierarchy of equations, through second order in ε:

$$\mathcal{O}(\varepsilon^0): \frac{\mathrm{d}^2 u_0}{\mathrm{d}z^2} = 1, \qquad -c(t) < z < 0, \tag{19}$$

$$\frac{\mathrm{d}^2 u_0}{\mathrm{d}z^2} - u_0 = 1, \qquad z > 0; \tag{20}$$

$$\mathcal{O}(\varepsilon^1): \frac{\partial^2 u_1}{\partial t^2} - \frac{\partial^2 u_1}{\partial z^2} = \frac{\mathrm{d}^2 c_1}{\mathrm{d}t^2}\frac{\mathrm{d}u_0}{\mathrm{d}z}, \qquad -c(t) < z < 0, \tag{21}$$

$$\frac{\partial^2 u_1}{\partial t^2} - \frac{\partial^2 u_1}{\partial z^2} + u_1 = \frac{\mathrm{d}^2 c_1}{\mathrm{d}t^2}\frac{\mathrm{d}u_0}{\mathrm{d}z}, \qquad z > 0; \tag{22}$$

$$\mathcal{O}(\varepsilon^2): \frac{\partial^2 u_2}{\partial t^2} - \frac{\partial^2 u_2}{\partial z^2} = 2\frac{\mathrm{d}c_1}{\mathrm{d}t}\frac{\partial^2 u_1}{\partial z \partial t} + \frac{\mathrm{d}^2 c_1}{\mathrm{d}t^2}\frac{\partial u_1}{\partial z} + \frac{\mathrm{d}^2 c_2}{\mathrm{d}t^2}\frac{\mathrm{d}u_0}{\mathrm{d}z} - \left(\frac{\mathrm{d}c_1}{\mathrm{d}t}\right)^2 \frac{\mathrm{d}^2 u_0}{\mathrm{d}z^2}, \qquad -c(t) < z < 0, \tag{23}$$

$$\frac{\partial^2 u_2}{\partial t^2} - \frac{\partial^2 u_2}{\partial z^2} + u_2 = 2\frac{\mathrm{d}c_1}{\mathrm{d}t}\frac{\partial^2 u_1}{\partial z \partial t} + \frac{\mathrm{d}^2 c_1}{\mathrm{d}t^2}\frac{\partial u_1}{\partial z} + \frac{\mathrm{d}^2 c_2}{\mathrm{d}t^2}\frac{\mathrm{d}u_0}{\mathrm{d}z} - \left(\frac{\mathrm{d}c_1}{\mathrm{d}t}\right)^2 \frac{\mathrm{d}^2 u_0}{\mathrm{d}z^2}, \qquad z > 0. \tag{24}$$

The boundary conditions associated with this hierarchy of equations are

$$\mathcal{O}(\varepsilon^0): u_0(-c_0) = U_0, \tag{25}$$

$$\mathcal{O}(\varepsilon^1): u_1(-c_0,t) = U_0\sin(\omega t) + c_1(t)\frac{\mathrm{d}u_0}{\mathrm{d}z}(-c_0), \tag{26}$$

$$\mathcal{O}(\varepsilon^2): u_2(-c_0,t) = c_2(t)\frac{\mathrm{d}u_0}{\mathrm{d}z}(-c_0) + c_1(t)\frac{\partial u_1}{\partial z}(-c_0,t) - \frac{1}{2}c_1(t)^2\frac{\mathrm{d}^2 u_0}{\mathrm{d}z^2}(-c_0), \tag{27}$$

at the left boundary of the whole domain. Note that this boundary condition is imposed only asymptotically. At the TDP we have $u_0(0) = u_1(0,t) = u_2(0,t) = 0$, and the continuity conditions (13) on the function and Eq. (14) on the derivatives have to hold at all orders.

From Eqs. (21)–(24), we see that the functions $u_1(z,t)$ and $u_2(z,t)$ obey non-homogeneous differential equations with the same associated homogeneous equations. As we shall see later on, this fact, which is well known, has an important consequence on the location of the resonant frequencies of the system.

Before we proceed further, we make the definition of the amplification factor, which will be used in the sequel, more precise.

3.1. The amplification factor D

As we mentioned in the Introduction, an important quantity used in this paper and of interest in the applications is the amplification factor D, which is the ratio of the oscillation amplitude of the TDP to the boundary oscillation at $z = -c(t)$.

In order to define D in a precise way, we begin by considering the truncated asymptotic expansion of $c(t)$ in series of ε:

$$\widetilde{c}_N(t) = \sum_{n=0}^{N} \varepsilon^n c_n(t). \tag{28}$$

Next, we define the excursions (or maximum elongations) of the TDP $c(t)$, of its coefficients $c_n(t)$ and of its truncated expansions $\widetilde{c}_N(t)$ over one period:

$$\Gamma(\varepsilon) = \frac{1}{2}\left[\max_{t\in[0,2\pi/\omega]} c(t) - \min_{t\in[0,2\pi/\omega]} c(t)\right], \tag{29}$$

$$\gamma_n = \frac{1}{2}\left[\max_{t\in[0,2\pi/\omega]} c_n(t) - \min_{t\in[0,2\pi/\omega]} c_n(t)\right], \tag{30}$$

$$\Gamma_N(\varepsilon) = \frac{1}{2}\left[\max_{t\in[0,2\pi/\omega]} \widetilde{c}_N(t) - \min_{t\in[0,2\pi/\omega]} \widetilde{c}_N(t)\right]. \tag{31}$$

Then, the function

$$D(U_0, \omega, \varepsilon) = \frac{\Gamma(\varepsilon)}{\varepsilon U_0} \tag{32}$$

is the *amplification factor*; it gives the measure of the amplification with which the oscillation at the boundary reflects on the oscillation of the TDP. It is easily seen (from Eqs. (16), (29) and (31)) that $\Gamma(\varepsilon)$ and $\Gamma_N(\varepsilon)$ are proportional to ε, and therefore the amplification factor D is of order zero in ε.

We would like to obtain first- and second-order asymptotic expressions for the amplification factor. One possible approach is that of defining the first- and second-order amplification factors from the amplitude of the oscillations of the expansion coefficients $c_1(t)$ and $c_2(t)$:

$$D_1'(U_0, \omega) = \frac{\gamma_1}{U_0}, \quad D_2'(U_0, \omega) = \frac{\gamma_2}{U_0}, \tag{33}$$

which leads to amplification factors which are independent of ε.

If we consider the definition (32) of the amplification factor and use the truncated expansions (28) for the TDP $c(t)$, we obtain expressions for the amplification factor which are correct through first or second order in ε:

$$D_1(U_0, \omega, \varepsilon) = \frac{\Gamma_1(\varepsilon)}{\varepsilon U_0}, \quad D_2(U_0, \omega, \varepsilon) = \frac{\Gamma_2(\varepsilon)}{\varepsilon U_0}. \tag{34}$$

Among these different amplification factors there exist two important relations:

(i) $D_1 = D_1'$ (so D_1 is independent of ε):

$$\begin{aligned} D_1 &= \frac{1}{2\varepsilon U_0}\left(\max_{t\in[0,2\pi/\omega]}[c_0 + \varepsilon c_1(t)] - \min_{t\in[0,2\pi/\omega]}[c_0 + \varepsilon c_1(t)]\right) \\ &= \frac{1}{2U_0}\left(\max_{t\in[0,2\pi/\omega]}[c_1(t)] - \min_{t\in[0,2\pi/\omega]}[c_1(t)]\right) = \frac{\gamma_1}{U_0} = D_1'. \end{aligned}$$

(ii) $D_1' + \varepsilon D_2'$ provides an upper bound for D_2:

$$\begin{aligned} D_2 &= \frac{1}{2\varepsilon U_0}\left(\max_{t\in[0,2\pi/\omega]}[c_0+\varepsilon c_1(t)+\varepsilon^2 c_2(t)] - \min_{t\in[0,2\pi/\omega]}[c_0+\varepsilon c_1(t)+\varepsilon^2 c_2(t)]\right) \\ &\leqslant \frac{1}{2U_0}\left[\max_{t\in[0,2\pi/\omega]}[c_1(t)] - \min_{t\in[0,2\pi/\omega]}[c_1(t)] \right. \\ &\quad \left. + \varepsilon\left(\max_{t\in[0,2\pi/\omega]}[c_2(t)] - \min_{t\in[0,2\pi/\omega]}[c_2(t)]\right)\right] \\ &= \frac{\gamma_1}{U_0} + \varepsilon\frac{\gamma_2}{U_0} = D_1' + \varepsilon D_2'. \end{aligned}$$

3.2. Zero-order solution

Eqs. (19) and (20), with the boundary conditions for u_0 given in Eq. (25) are easily integrated, giving

$$u_0(z) = z\left(\frac{c_0+z}{2} - \frac{U_0}{c_0}\right), \quad -c_0 < z < 0, \tag{35}$$

$$u_0(z) = \mathrm{e}^{-z} - 1, \quad z > 0. \tag{36}$$

It is easy to see that these two expressions define the same function given by the steady-state equations in the original variables, provided that the identification $x = c_0 + z$ between the new and the old variables is made, namely $u_S(x) = u_0(x - c_0)$. The value of c_0 is then obtained by using the continuity condition on the derivative, Eq. (14), and is consistent with Eq. (6).

3.3. First-order solution

The first-order solution was already obtained in Ref. [2] by using the transformation (7). The same results are obtained (to the first order and up to the different $\sqrt{2}$ factor used in the dimensionless variable x) with the transformation (8). They are summarized here for clarity.

By substituting the expansions (17)–(18) for u_1 and c_1 in Eqs. (21) and (22), and then equating separately to zero the coefficient of $\cos(n\omega t)$ and $\sin(n\omega t)$ for each n, we obtain an infinite set of equations from which the expansion coefficients $f_{1n}(z)$, $g_{1n}(z)$, a_{1n} and b_{1n} are determined. Actually, only $f_{11}(z)$, $g_{11}(z)$, a_{11} and b_{11} are different from zero. The calculations are rather long and we carried them out with a symbolic manipulation program. We report only the governing equation of $f_{11}(z)$,

$$\frac{\mathrm{d}^2 f_{11}}{\mathrm{d}z^2} + \omega^2 f_{11} + \left(\frac{U_0}{c_0} - \frac{c_0}{2} - z\right)\omega^2 a_{11} = 0, \quad z < 0, \tag{37}$$

$$\frac{\mathrm{d}^2 f_{11}}{\mathrm{d}z^2} + (\omega^2 - 1) f_{11} + \omega^2 \mathrm{e}^{-z} a_{11} = 0, \quad z > 0, \tag{38}$$

which shows that the solutions of Eq. (38) depend crucially upon ω [2]: the two linearly independent solutions of the associated homogeneous equation are hyperbolic if $\omega < 1$ (“1-subcritical” regime) and oscillatory if $\omega > 1$ (“1-supercritical” regime). In the 1-subcritical regime, the boundary conditions that the solution be bounded as $z \to \infty$ must be used, while in the 1-supercritical case we must ensure that there are no traveling waves returning from infinity.

1-Subcritical regime ($\omega < 1$): By imposing the non-homogeneous boundary conditions at $z = -c_0$ and by matching the left and right derivatives at $z = 0$, we find that f_{11} and a_{11} are the only non-vanishing contributions to the solution for $u_1(z,t)$ and $c_1(t)$; therefore we obtain

$$u_1(z,t) = f_{11}(z)\sin(\omega t), \tag{39}$$

$$c_1(t) = a_{11}\sin(\omega t), \tag{40}$$

where $f_{11}(z)$ is the solution of Eqs. (37) and (38) with the assigned boundary conditions, and vanishes exponentially as $z \to \infty$; the coefficient a_{11} is then determined by the continuity condition on $\mathrm{d}f_{11}(z)/\mathrm{d}z$ at $z = 0$. We have:

$$a_{11} = \frac{U_0\omega}{\sqrt{1-\omega^2}\sin(\omega c_0) + \omega\cos(\omega c_0)}. \tag{41}$$

1-Supercritical regime ($\omega > 1$): In this case both f_{11} and g_{11} are different from zero, and in the range $z > 0$ the solution, which now supports right-traveling waves, can be written in the form

$$\begin{aligned} u_1(z,t) = {} & \alpha_{11}\sin(\omega t - z\sqrt{\omega^2-1}) + \alpha_{12}\cos(\omega t - z\sqrt{\omega^2-1}) \\ & + \tilde{f}_{11}(z)\sin(\omega t) + \tilde{g}_{11}(z)\cos(\omega t), \end{aligned} \tag{42}$$

where $\tilde{f}_{11}(z)$ and $\tilde{g}_1(z)$ decay exponentially for $z \to \infty$. In the range $-c(t) < z < 0$ there are also left-traveling waves, which are due to the reflection at the TDP of the right-traveling waves generated at $z = -c(t)$. We further have

$$c_1(t) = a_{11}\sin(\omega t) + b_{11}\cos(\omega t), \tag{43}$$

with a_{11} and b_{11} given by

$$a_{11} = \frac{U_0\omega^2\cos(\omega c_0)}{\omega^2 - \sin^2(\omega c_0)}, \quad b_{11} = \frac{U_0\omega\sqrt{\omega^2-1}\sin(\omega c_0)}{\omega^2 - \sin^2(\omega c_0)}. \tag{44}$$

Note that the presence of the cosine terms means that in this case there is a phase shift between the excitation and the motion of the cable.

At the first order in ε, we have $\gamma_1 = |a_{11}|$ in the 1-subcritical case, and $\gamma_1 = \sqrt{a_{11}^2 + b_{11}^2}$ in the 1-supercritical case. The first-order amplification factor D_1' is therefore given by

$$D_1' = \frac{|a_{11}|}{U_0} = \frac{\omega}{|\sqrt{1-\omega^2}\sin(\omega c_0) + \omega\cos(\omega c_0)|} \tag{45}$$

in the 1-subcritical case and by

$$D_1' = \frac{\sqrt{a_{11}^2 + b_{11}^2}}{U_0} = \frac{\omega}{\sqrt{\omega^2 - \sin^2(\omega c_0)}} \tag{46}$$

in the 1-supercritical case. $D_1'(\omega)$ is reported in Fig. 2 for three different values of c_0. The results show the presence of (primary) resonances, given by the solutions of

$$\tan(\omega c_0) = -\frac{\omega}{\sqrt{1-\omega^2}} \tag{47}$$

(see Eq. (45)), all lying in the 1-subcritical region, and whose number increases with increasing U_0 or c_0. In fact, a resonant-like behaviour is observed also in the 1-supercritical region, although the peaks are not pronounced and although there are no ideal resonance because the equation $\omega = \sin(\omega c_0)$ (see Eq. (46)) has no solution for $\omega > 1$. This is due to the fact that in the 1-supercritical regime energy is lost by radiation at infinity, so that the system experiences dissipation, which is responsible for the reduction of the peaks of the resonance curve, as in classical damped oscillators.

4. Second-order solution

We obtain the second-order solution by substituting the expansions (17) and (18) for u_2 and c_2 in Eqs. (23) and (24), and then equating separately to zero the coefficient of $\cos(n\omega t)$ and $\sin(n\omega t)$ for each n. The functions $f_{2n}(z)$ and $g_{2n}(z)$ satisfy non-homogeneous second-order differential equations, in which the known term is

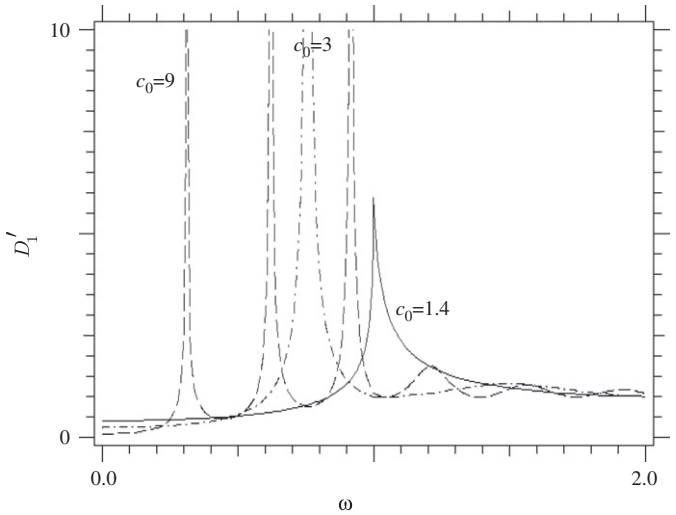

Fig. 2. $D_1'(\omega)$ for three different values of c_0.

proportional to some of the coefficients a_{2n} and b_{2n}, and are equipped with boundary conditions similar to the ones of the first-order solution, though slightly more complicated.

For simplicity, we show here only the differential equation governing $g_{22}(z)$:

$$\frac{\mathrm{d}^2 g_{22}}{\mathrm{d}z^2}(z) + 4\omega^2 g_{22}(z) - \frac{3U_0\omega^3 \cos(z\omega)\csc(\omega c_0)a_{11}}{2} + \left[1 + \frac{3}{4}\left(2\frac{U_0}{c_0} - c_0\right)\omega\cos(\omega(z+c_0))\csc(\omega c_0)\right]\omega^2 a_{11}^2 + (4U_0 - 4z - 2c_0)b_{22} = 0, \quad z<0, \tag{48}$$

$$\frac{\mathrm{d}^2 g_{22}}{\mathrm{d}z^2} + (4\omega^2 - 1)g_{22}(z) + \frac{1}{2}\left[8b_{22} + \left(1 - \frac{3}{2}v\right)a_{11}^2\right]\omega^2 \mathrm{e}^{-z} + \frac{3}{2}v(\mathrm{e}^{-z} - \mathrm{e}^{-zv})\omega^2 a_{11}^2 = 0, \quad z>0, \tag{49}$$

$$v = \sqrt{|\omega^2 - 1|}; \tag{50}$$

the other coefficients obey differential equations with a similar structure.

We notice that the solutions of Eq. (49) depend crucially upon ω: the two linearly independent solutions of the associated homogeneous equation are hyperbolic if $\omega<\frac{1}{2}$ (''2-subcritical'' regime) and oscillatory if $\omega>\frac{1}{2}$ (''2-supercritical'' regime). This shows that the transition between subcritical and supercritical regimes, which happens at $\omega = 1$ in the first-order solution, here occurs at $\omega = \frac{1}{2}$.

From the previous considerations, we can infer that the threshold frequency between subcritical and supercritical behaviour is different at different orders of ε, and is given by $\omega = 1/n$ for the n-th order solution. This is a consequence of the fact that the homogeneous equations associated with the differential equations of the hierarchy (see Eqs. (21)–(24)) are the same. The result is that for *every* value of the excitation frequency there is always an infinite number of traveling waves, which is one of the main consequences of the nonlinearity of the problem. However, when ω is small enough, these waves are of high order and then their amplitudes are small, and negligible from a practical point of view.

2-Subcritical regime ($\omega<\frac{1}{2}$): Due to the boundary conditions, we have that the only non-vanishing contributions to the solution for $u_2(z,t)$ and $c_2(t)$ are

$$u_2(z,t) = g_{20}(z) + g_{22}(z)\cos(2\omega t), \tag{51}$$

$$c_2(t) = b_{20} + b_{22}\cos(2\omega t), \tag{52}$$

where $g_{20}(z)$ and $g_{22}(z)$ are the solutions of differential equations similar to Eqs. (48) and (49) with the assigned boundary conditions, and decay exponentially as $z \to \infty$. The coefficients b_{20} and b_{22} are then determined by the continuity condition on the derivatives at $z = 0$; they are reported in Appendix A.

From expression (A.2) we note that in this range there are secondary resonances, which add to primary resonances, and which are solutions of

$$\tan(2\omega c_0) = -\frac{2\omega}{\sqrt{1-4\omega^2}}; \tag{53}$$

by comparison with Eq. (47), we see that the secondary resonances ω_2 occur at values of ω just one half of the primary resonances ω_1. From this result, it is immediate to infer that the resonances of order n are just given by $\omega_n = \omega_1/n$.

The presence of secondary resonances is the main, non-negligible effect highlighted by the second-order terms, which is missed by the first-order analysis. However, since the first- and the second-order solutions are both decaying functions for $z \to \infty$, we have that, *far enough* from the secondary resonances, the effects of the second-order terms are negligible in this range. By anticipating the results of the following sub-section, it is expected that the third-order terms could be important for $1 < \omega < \frac{1}{2}$, and so on.

2-Supercritical regime ($\omega > 1$)*:* For these values of ω, terms proportional to $\sin(2\omega t)$ are also present in the solution; therefore we have

$$u_2(z,t) = g_{20}(z) + g_{22}(z)\cos(2\omega t) + f_{22}(z)\sin(2\omega t), \tag{54}$$

$$c_2(t) = b_{20} + b_{22}\cos(2\omega t) + a_{22}\sin(2\omega t). \tag{55}$$

In the range $z > 0$ the equation supports right-traveling waves and the solution can be expressed in the form

$$\begin{aligned} u_2(z,t) = {} & \alpha_{21}\sin(2\omega t - z\sqrt{4\omega^2-1}) + \alpha_{22}\cos(2\omega t - z\sqrt{4\omega^2-1}) \\ & + \tilde{g}_{20}(z) + \tilde{g}_{22}(z)\cos(2\omega t) + \tilde{f}_{22}(z)\sin(2\omega t), \end{aligned} \tag{56}$$

where $\tilde{g}_{20}(z)$, $\tilde{g}_{22}(z)$ and $\tilde{f}_{22}(z)$ are functions which decay exponentially as $z \to \infty$.

From Eqs. (42) and (56) we infer that each wave travels with a different velocity. More precisely, the propagation velocity of the wave of order n is

$$v_n = \frac{\omega}{\sqrt{\omega^2 - 1/n^2}}, \tag{57}$$

so that the most important part of the solution (the one which does not decay for $z \to \infty$) is the superposition of waves of different speeds.

The expressions of b_{20}, b_{22} and a_{22} are reported in Appendix A. With these formulas we draw some examples of the TDP motion (Fig. 3). Fig. 3(a) corresponds to a 1-subcritical, 2-supercritical regime ($\frac{1}{2} < \omega < 1$), while Fig. 3(b) corresponds to a 1-supercritical, 2-supercritical regime ($\omega > 1$). We see that the difference between the first- and the second-order solutions is important but not dramatic in the case of Fig. 3(a), where the supercritical terms are present in the second-order solution only; much larger differences between the first- and second-order TDP motions appear in Fig. 3(b), where the supercritical terms are present at both orders. Here the effects of the second-order terms are dominant, even for that relatively small value of ε.

By the expressions reported in Appendix A we see that there could be resonances for $\frac{1}{2} < \omega < 1$ iff $D(\omega) = 0$, and there could be resonances for $\omega > 1$ iff $D_A(\omega) = 0$ or $D_B(\omega) = 0$. As these equations have no solutions in those ranges, we reiterate the same conclusion obtained for the first-order terms, namely, the presence of traveling waves in the supercritical regimes eliminates the ideal resonances.

In order to further illustrate the effect of the second-order terms in the asymptotic solution, in Fig. 4 we show the profiles of the solution $u(x,t)$ through zero-, first- and second-order in ε at four different times, corresponding to $\omega t_1 = 0$, $\omega t_2 = \pi/4$, $\omega t_3 = \pi/2$ and $\omega t_4 = 3\pi/4$. Figs. 4(a) and (b) show the first- and the second-order solutions respectively, for $\omega = 0.9$, $c_0 = 1.9$ and $\varepsilon = 0.1$. Here, the first-order solution is in the subcritical regime while the second-order solution is in the supercritical regime. We observe second-order

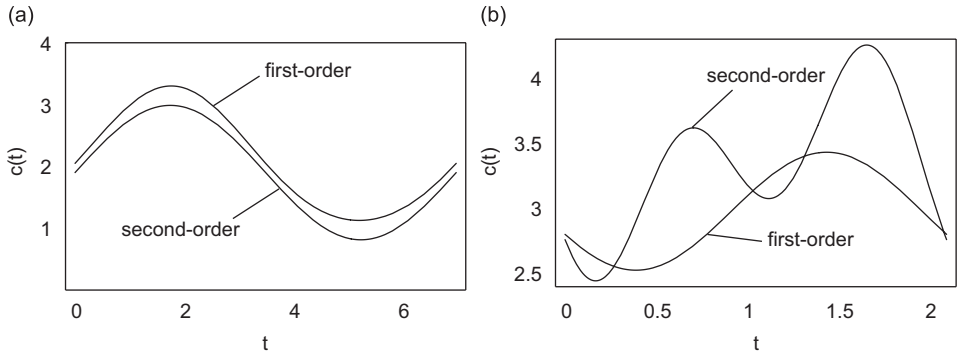

Fig. 3. First- and second-order motions of the TDP for (a) $\omega = 0.9$, $c_0 = 1.9$ and $\varepsilon = 0.1$; (b) $\omega = 3.0$, $c_0 = 3.0$ and $\varepsilon = 0.06$.

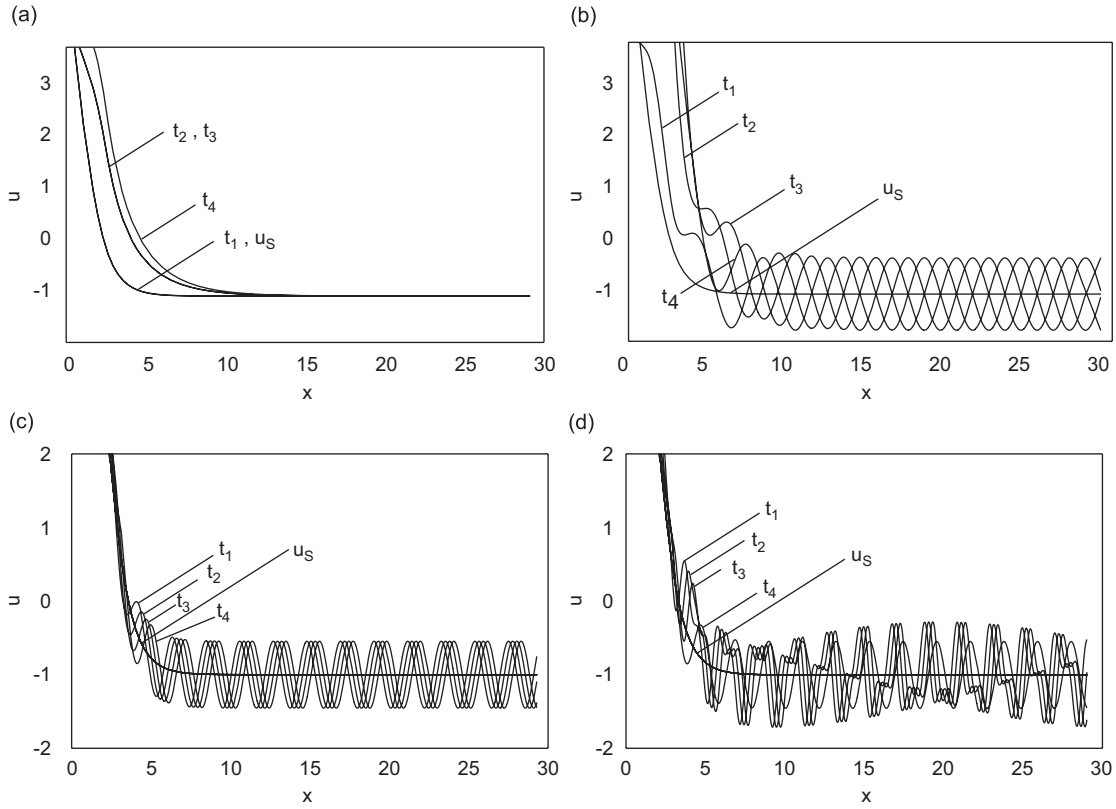

Fig. 4. First-(a),(c) and second-order (b),(d) profiles at four different times, corresponding to $\omega t_1 = 0$, $\omega t_2 = \pi/4$, $\omega t_3 = \pi/2$ and $\omega t_4 = 3\pi/4$. The static profiles are also shown. (a) and (b) $\omega = 0.9$, $c_0 = 1.9$ and $\varepsilon = 0.1$; (c) and (d) $\omega = 3.0$, $c_0 = 3.0$ and $\varepsilon = 0.06$.

waves propagating towards infinity, and the difference between the first- and the second-order solutions is large, even at this small value of ε.

Figs. 4(c) and (d) show the first- and the second-order solutions for $\omega = 3$, $c_0 = 3$ and $\varepsilon = 0.06$. Here, both the first and the second-order solutions are in the supercritical regime, giving origin to first- and second-order propagating waves. These waves propagate with different velocity (see Eq. (57)), so that there is an interaction, which is clearly visible in Fig. 4(d), and which further shows the importance of the second-order terms.

4.1. Second-order shift and second-order amplification factors

An important property of the second-order solution is that $c(t)$ now oscillates about an average position which is shifted with respect to the static TDP c_0. This shift, which was not present in the first-order solution, is given by the coefficient b_{20} and is shown in Fig. 5 for three different values of c_0. Note that b_{20} has the same resonances of the first-order solution, and that it tends to a constant value for $\omega \to \infty$.

At the second order in ε, we have $\gamma_2 = |b_{22}|$ in the subcritical case, and $\gamma_2 = \sqrt{a_{22}^2 + b_{22}^2}$ in the supercritical case. The second-order amplification factor D_2' is therefore given by

$$D_2'(U_0, \omega) = \frac{|b_{22}|}{U_0} \tag{58}$$

in the 2-subcritical case and by

$$D_2'(U_0, \omega) = \frac{\sqrt{a_{22}^2 + b_{22}^2}}{U_0} \tag{59}$$

in the 2-supercritical case (see Appendix A for the expressions of a_{22} and b_{22}).

In Fig. 6 we show the second-order amplification factors D_2 and $D_1' + \varepsilon D_2'$ as functions of ω for the same three values of c_0 of Figs. 2 and 5. For the sake of comparison, also the first-order amplification factor $D_1' = D_1$ is reported.

The first important aspect highlighted in Fig. 6 is the confirmation of the occurrence, in the range $\omega < \frac{1}{2}$, of superharmonic resonances which are added, at the second-order, to the primary first-order resonances. The superharmonic resonances, being of "secondary" type, are sometimes less pronounced than the primary ones. In fact, one is clearly visible at $\omega \simeq 0.45$ in Fig. 6(c), another one at $\omega \simeq 0.37$ in Fig. 6(b), while other resonances result in only very small peaks, which can be missed at a first glance (see in particular at $\omega \simeq 0.49$ in Fig. 6(a)).

In the range $\omega > 1$ the second-order terms increase the amplitude of the first-order peaks, confirming how they can effectively be associated to a resonant-like (damped) behaviour.

Confirming in a systematic way the anticipation of the previous section, we see from Figs. 3–6 that the second-order terms are

(i) important for $0 < \omega < \frac{1}{2}$ (1-subcritical and 2-subcritical regime). In this regime they highlight the presence of superharmonic resonances, not evidenced by the first-order solution. Far from the secondary

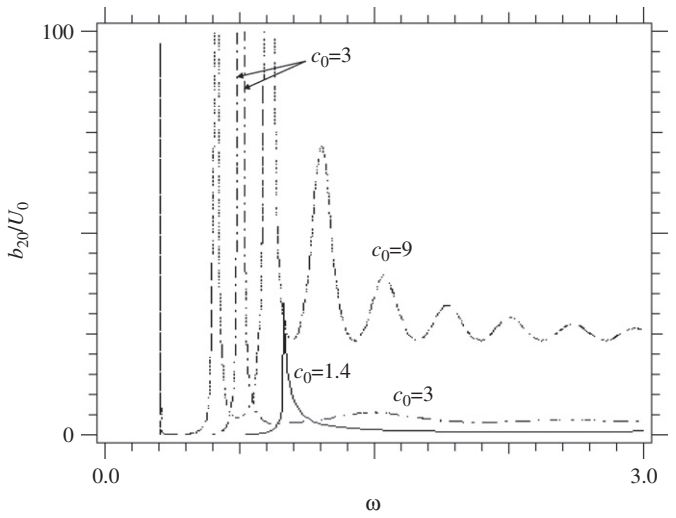

Fig. 5. Second-order shift b_{20} for three different values of c_0.

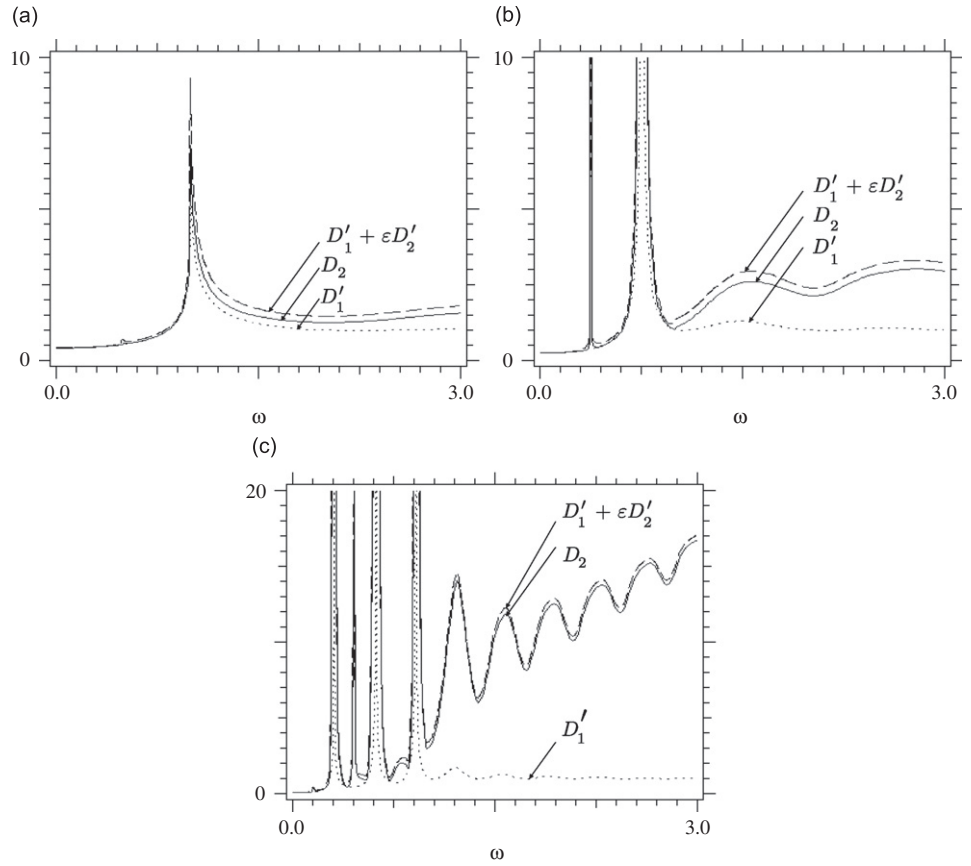

Fig. 6. Second-order amplification factors D_2 and $D_1' + \varepsilon D_2'$ and first-order amplification factor D_1' for $\varepsilon = 0.2$ and for three different values of c_0: (a) $c_0 = 1.4$, (b) $c_0 = 3$ and (c) $c_0 = 9$.

resonance, however, the second-order terms quantitatively do not add important contributions to the first-order solution;

(ii) very important for $\frac{1}{2} < \omega < 1$ (1-subcritical and 2-supercritical regime). Here they contribute in non-negligible manner to the TDP motion even far from the resonances. Furthermore, far from the TDP they represent the dominant part of the cable dynamics;

(iii) fundamental for $1 < \omega$ (1-supercritical and 2-supercritical regime), where linear terms completely miss the TDP response of the system. This importance is c_0 dependent, and becomes dramatic for large values of c_0 (see in particular Fig. 6(c) and note that it has a different vertical scale). In contrast, in this regime the influence on the cable dynamics is relevant but less important than in the previous case.

The effect of the other governing parameter c_0 is also remarkable. In particular, the second-order terms become more and more important for large values of c_0; in the case of Fig. 6(c), for example, the differences between first- and second-order solutions are so marked that even the second-order solution is no longer accurate for that value of ε. The differences are important also in the case of Fig. 6(b).

A surprising result is seen in Fig. 6: the second-order amplification factors increase, on average, with the frequency as ω becomes larger than 1. This fact, which is in agreement with the numerical results for the beam equation presented in Ref. [3], calls for a different asymptotic solution for large values of ω, where $1/\omega$ should be the appropriate smallness parameter. This issue, however, is out of the scopes of the present paper an will be left for future work.

As far as the comparison between different second-order amplification factors is concerned, we note that both D_2 and $D_1' + \varepsilon D_2'$ share the same qualitative behaviour, and they differ for an almost constant value. Thus, both are reliable measures of the second-order effects in the system dynamics.

5. Numerical results and comparisons

In this section we show some preliminary numerical simulations of our model equations, which we have produced by using a straightforward finite difference algorithm. The aim of these simulations is limited to the validation of our approximate analytical solution; in order to perform more systematic simulations, several issues concerning the numerics need further study. In particular, the problem of imposing the boundary conditions at the infinite end of the domain is very difficult, and in the simulations presented here the time evolution is simply stopped as the propagating waves reach the cutoff boundary, taken sufficiently large. The detailed study of this and other issues concerning the numerical solution of the equations is left for future work.

In Fig. 7 we show the time evolution of the solution $u(x,t)$, for $0 \leqslant x \leqslant 150$ at four different times, (a) $t = 50$, (b) $t = 100$, (c) $t = 150$ and (d) $t = 200$, for $\omega = 1.2$, which sets the system in the 1-supercritical regime. The initial condition used here is $u(x,0) = u_S(x)$ with $\partial u/\partial t(x,0) = 0$, that is we initialize the system at the static profile with no initial velocity. We also have $c_0 = 1.4$ and $\varepsilon = 0.1$. We see clearly a large amplitude wave which propagates towards infinity, as predicted by our theoretical analysis.

In Figs. 8(a) and (b), we look at the motion of the TDP over one period, by comparing the first- and second-order analytical expressions with the numerical results. Fig. 8(a) refers to the 1-subcritical, 2-supercritical regime (we have chosen $\omega = 0.7$ for this case) while Fig. 8(b) refers to the 1-supercritical, 2-supercritical regime (here we have $\omega = 1.2$). In both cases, we have $c_0 = 1.4$, while $\varepsilon = 0.4$ in Fig. 8(a) and $\varepsilon = 0.1$ in Fig. 8(b). We note the difference between the first- and the second-order asymptotic approximations in both cases, which

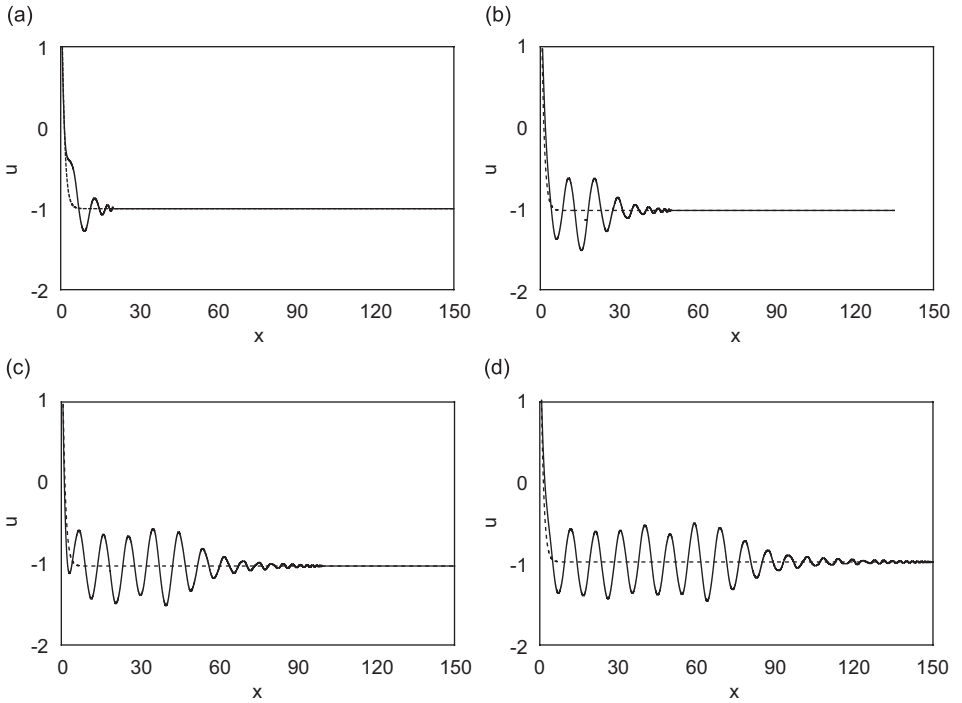

Fig. 7. Numerical simulation of a propagating wave for $\omega = 1.2$, $c_0 = 1.4$ and $\varepsilon = 0.1$ at four different times: (a) $t = 50$, (b) $t = 100$, (c) $t = 150$ and (d) $t = 200$. The solid line represents the numerical solution of the model equations, the dashed line represents the static profile.

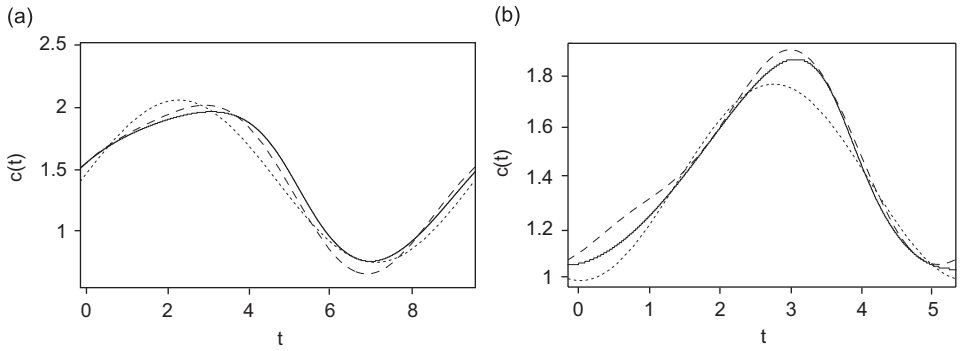

Fig. 8. Time behaviour of the TDP over one period for (a) $\omega = 0.7$, $c_0 = 1.4$ and $\varepsilon = 0.4$ and (b) $\omega = 1.2$, $c_0 = 1.4$ and $\varepsilon = 0.1$; first-(short dashed line) and second-order (long dashed line) asymptotic result and (solid line) numerical result.

demonstrates the importance of the second-order analysis. Also, we see that the second-order analytical solution reproduces the numerical results very well, even for the rather large value of ε chosen in Fig. 8(a).

6. Conclusions and outlook

This work is a continuation of our study of the nonlinear dynamics of semi-infinite cables resting on a unilateral elastic substrate by means of a straightforward perturbative approach. We have investigated periodic solutions around the static profile.

At each order in our perturbation scheme, two different regimes have been identified, one below (called subcritical) and one above (called supercritical) a certain critical excitation frequency (called cutoff frequency). In the latter, energy is lost by radiation at infinity, while in the former this phenomenon does not occur. On the contrary, in the subcritical regime various resonances are observed; their number depends on the static configuration around which the system performs nonlinear oscillations and they are absent, or better, less pronounced in the supercritical regime, due to the dissipation by radiation. The cutoff frequency ω_n at the n-th order is given by $\omega_n = 1/n$. Therefore, for any value of the frequency of the forcing oscillation, there will be a supercritical regime at some order in the perturbation expansion. That is to say, waves will always propagate towards infinity, with smaller and smaller amplitude as $\omega \to 0$.

The first-order solution gives the linear response of the system to the external excitation, while nonlinear effects start appearing at the second order and higher. In particular, the appearance of superharmonic resonances has been highlighted. The results are illustrated both by showing the spatial shape of the excitation and by the amplification factor D, which better summarizes the main features of the solution.

It should be remarked that the perturbative approach proposed in this work can only catch certain nonlinear phenomena, while others, such as the bending of the resonance curves near resonant frequencies and hysteresis cycles, need a different asymptotic analysis. In order to describe these effects, a detuning parameter should be introduced near the resonant frequencies and a multiple-scale analysis should be performed. Some aspects of the solution, like the increasing of the second-order amplification factor with the excitation frequency ω for $\omega > 1$, indicate that the problem might be a singular perturbation problem. For a fixed frequency ω and away from resonances, however, we believe that this is not the case; the convergence with respect to ε is non-uniform only when the limits $\varepsilon \to 0$ and $\omega \to \infty$ are considered simultaneously.

To assess the validity of our asymptotic analytical approach, a comparison with some numerical simulations has been performed, both in terms of the TDP motion and of the beam motion. Both 1-supercritical and 1-subcritical cases are considered, and it is shown that the analytical solutions are in very good agreement with the numerical simulations.

Among many others, at least one development of the present paper is worthy and left for future works. It is the determination of the range of stability of the considered periodic solution, which has both practical and theoretical interest, as the eigenvalues behaviour is expected to be influenced by the unboundedness of the domain.

Appendix A. Second-order coefficients

We report here the explicit expressions for the second-order coefficients a_{22}, b_{22} and b_{20} of the TDP motion $c(t) = c_0 + \varepsilon[a_{11}\sin(\omega t) + b_{11}\cos(\omega t)] + \varepsilon^2[b_{20} + a_{22}\sin(2\omega t) + b_{22}\cos(2\omega t)] + \ldots$ (the first-order coefficients are given by Eqs. (41) and (44)). We recall that c_0 and U_0 are related by $c_0 = \sqrt{1+2U_0} - 1$. In the following, we use the definitions $v = \sqrt{|\omega^2 - 1|}$ and $\mu = \sqrt{|4\omega^2 - 1|}$.

1-subcritical and 2-subcritical regimes: $\omega < \frac{1}{2}$

$$a_{22} = 0, \tag{A.1}$$

$$b_{22} = B_1(\omega)a_{11} + B_2(\omega)a_{11}^2, \tag{A.2}$$

$$b_{20} = B_3(\omega)a_{11} + B_4(\omega)a_{11}^2, \tag{A.3}$$

with

$$B_1(\omega) = \frac{U_0\omega^2\cot(2\omega c_0)\csc(\omega c_0)}{\mu + 2\omega\cot(2\omega c_0)}, \tag{A.4}$$

$$B_2(\omega) = \frac{-1 - \mu + 2\mu v - \omega\cos(2\omega c_0)\csc(\omega c_0)(2\omega\csc(\omega c_0) + \sec(\omega c_0))}{4(\mu + 2\omega\cot(2\omega c_0))}, \tag{A.5}$$

$$B_3(\omega) = -\frac{U_0\omega\csc(\omega c_0)c_0}{2U_0 + c_0^2}, \tag{A.6}$$

$$B_4(\omega) = \frac{U_0\omega}{2U_0 + c_0^2}\cot(\omega c_0) + \frac{(1 + 2U_0\omega^2)c_0}{2(2U_0 + c_0^2)} - \frac{\omega^2 c_0^3}{2(2U_0 + c_0^2)}, - \frac{\omega(2v\omega + (1+v)\cot(\omega c_0))c_0^2}{2(1+v)(2U_0 + c_0^2)}. \tag{A.7}$$

1-subcritical and 2-supercritical regimes: $\frac{1}{2} < \omega < 1$

$$a_{22} = A_1(\omega)a_{11} + A_2(\omega)a_{11}^2, \tag{A.8}$$

$$b_{22} = B_1(\omega)a_{11} + B_2(\omega)a_{11}^2, \tag{A.9}$$

with

$$A_1(\omega) = -2U_0\mu\omega^2\cos(\omega c_0)\cos(2\omega c_0)N_A(\omega), \tag{A.10}$$

$$A_2(\omega) = \mu\cos(\omega c_0)((1+\omega^2)\cos(\omega c_0) - v^2\cos(3\omega c_0) + v\omega(\sin(\omega c_0) + \sin(3\omega c_0)))N_A(\omega) \tag{A.11}$$

and

$$B_1(\omega) = \frac{U_0\omega^3\csc(\omega c_0)}{D(\omega)}, \tag{A.12}$$

$$B_2(\omega) = (-\omega\cos(2\omega c_0) - 2\omega^3\cos^2(2\omega c_0)\csc^2(\omega c_0) + (\tfrac{1}{2} - v - 2\omega^2 + 4v\omega^2)\sin(2\omega c_0) - \tfrac{1}{2}\omega^2\csc(2\omega c_0))\sin(2\omega c_0)N_B(\omega), \tag{A.13}$$

with

$$D(\omega) = 8\omega^2 - 1 + \cos(4\omega c_0), \tag{A.14}$$

$$N_A(\omega) = \frac{c_0^2}{(c_0 - U_0)D(\omega)}, \tag{A.15}$$

$$N_B(\omega) = \frac{\sin(2\omega c_0)}{(c_0 - U_0)D(\omega)}. \tag{A.16}$$

The second-order shift coefficient b_{20} has the same expression as in the *1-subcritical and 2-subcritical regimes* for $\omega<1$ (see Eqs. (A.3), (A.6) and (A.7)).

1-supercritical and 2-supercritical regime: $\omega>1$

$$a_{22} = \frac{A_1(\omega)a_{11} + A_2(\omega)b_{11} + A_3(\omega)a_{11}^2 + A_4(\omega)b_{11}^2 + A_5(\omega)a_{11}b_{11}}{D_A(\omega)}, \tag{A.17}$$

$$b_{22} = \frac{B_1(\omega)a_{11} + B_2(\omega)b_{11} + B_3(\omega)a_{11}^2 + B_4(\omega)b_{11}^2 + B_5(\omega)a_{11}b_{11}}{D_B(\omega)}, \tag{A.18}$$

$$b_{20} = \frac{B_6(\omega)a_{11} + B_7(\omega)a_{11}^2 + B_8(\omega)b_{11}^2}{2(2U_0 + c_0^2)}, \tag{A.19}$$

with

$$\begin{aligned} D_A(\omega) = {} & 4U_0^2\omega^2 \cot(2\omega c_0)\csc(\omega c_0)^2 \sin(4\omega c_0) \\ & + 4(2\mu^2 - U_0\omega^2 \cot(2\omega c_0)\csc(\omega c_0)^2 \sin(4\omega c_0))c_0^2, \\ & + \omega^2 \cot(2\omega c_0)\csc(\omega c_0)^2 \sin(4\omega c_0)c_0^4, \end{aligned} \tag{A.20}$$

$$A_1(\omega) = -2U_0\mu\omega^2(1 + 2\cos(\omega c_0))\sec\left(\frac{\omega c_0}{2}\right)^2 \sec(\omega c_0)c_0^2, \tag{A.21}$$

$$A_2(\omega) = -2U_0\omega^3 \cos(2\omega c_0)^2 \csc(\omega c_0)^3 c_0(2U_0 - c_0^2), \tag{A.22}$$

$$\begin{aligned} A_3(\omega) = {} & 2\mu c_0\left(2U_0\omega\left(3\cot(2\omega c_0) + \omega\left(2 + \sec\left(\frac{\omega c_0}{2}\right)^2 \sec(\omega c_0)\right)\right)\right. \\ & \left. - \omega\left(3\cot(2\omega c_0) + \omega\left(2 + \sec\left(\frac{\omega c_0}{2}\right)^2 \sec(\omega c_0)\right)\right)c_0^2 + c_0(3 + 4v(-\mu + v) + 4\omega\tan(\omega c_0))\right), \end{aligned} \tag{A.23}$$

$$\begin{aligned} A_4(\omega) = {} & 4\mu c_0(2U_0\omega(\omega \cot(\omega c_0)^2 - \cot(2\omega c_0)) \\ & + c_0(-1 + 2(\mu - v)v + 2\omega \cot(2\omega c_0) \\ & + \omega(-(\omega \cot(\omega c_0)^2) + \cot(2\omega c_0))c_0)), \end{aligned} \tag{A.24}$$

$$\begin{aligned} A_5(\omega) = {} & 2U_0^2\omega^3 \cos(2\omega c_0)(3 - 2\cos(\omega c_0) + \cos(4\omega c_0))\csc(\omega c_0)^3 \sec(\omega c_0) \\ & + 4U_0\omega \cot(2\omega c_0)(-2 + 4(\mu - v)v + 2\omega \cot(\omega c_0) - 2\omega \sin(2\omega c_0))c_0 \\ & + (4\mu^2 + 2U_0\omega^3 \cos(2\omega c_0)\csc(\omega c_0)^3(2 - (3 + \cos(4\omega c_0))\sec(\omega c_0)))c_0^2 \\ & - 4\omega \cot(2\omega c_0)(-1 + 2(\mu - v)v + \omega \cot(\omega c_0) - \omega \sin(2\omega c_0))c_0^3 \\ & + \omega^3(3 - 2\cos(\omega c_0) + \cos(4\omega c_0))\cot(2\omega c_0)\csc(\omega c_0)^2 c_0^4, \end{aligned} \tag{A.25}$$

$$D_B(\omega) = -64\mu^2 c_0^2 - 8\omega^2 \cot(2\omega c_0)\csc(\omega c_0)^2 \sin(4\omega c_0)(2U_0 - c_0^2)^2, \tag{A.26}$$

$$B_1(\omega) = 4U_0\omega^3(1 + 2\cos(\omega c_0))\cos(2\omega c_0)\csc\left(\frac{\omega c_0}{2}\right)\sec\left(\frac{\omega c_0}{2}\right)^3 c_0(2U_0 - c_0^2), \tag{A.27}$$

$$B_2(\omega) = -16U_0\mu\omega^2(\cos(\omega c_0) + \cos(3\omega c_0))\csc(\omega c_0)^2 c_0^2, \tag{A.28}$$

$$B_3(\omega) = 48\mu^2 c_0^2 + \omega \csc(\omega c_0)^2 \sin(4\omega c_0)(2U_0 - c_0^2)\left(-8U_0\omega^2\left(1 + 2\csc(2\omega c_0)\tan\left(\frac{\omega c_0}{2}\right)\right)\right.$$
$$\left. +4\omega^2 c_0^2\left(1 + 2\csc(2\omega c_0)\tan\left(\frac{\omega c_0}{2}\right)\right) - 2c_0(3 + 4\nu(-\mu + \nu) + 4\omega\tan(\omega c_0))\right), \quad \text{(A.29)}$$

$$B_4(\omega) = -32\mu^2 c_0^2 + 4\omega \csc(\omega c_0)^2 \sin(4\omega c_0)(2U_0 - c_0^2)(-2U_0\omega^2 \cot(\omega c_0)^2$$
$$+ c_0(1 + 2\nu(-\mu + \nu) - 2\omega\cot(2\omega c_0) + \omega^2 \cot(\omega c_0)^2 c_0)), \quad \text{(A.30)}$$

$$B_5(\omega) = 4\mu c_0(-2U_0\omega \csc(\omega c_0)^2(4\omega\cos(\omega c_0) - 2\omega(3 + \cos(4\omega c_0)) + \sin(4\omega c_0))$$
$$+ 8(-1 + 2(\mu - \nu)\nu + \omega\cot(\omega c_0) - \omega\sin(2\omega c_0))c_0$$
$$+ \omega \csc(\omega c_0)^2(4\omega\cos(\omega c_0) - 2\omega(3 + \cos(4\omega c_0)) + \sin(4\omega c_0))c_0^2) \quad \text{(A.31)}$$

and

$$B_6(\omega) = -2U_0\omega c_0 \tan\left(\frac{\omega c_0}{2}\right), \quad \text{(A.32)}$$

$$B_7(\omega) = \omega^2 c_0(2U_0 - c_0^2) - \omega(2U_0 - c_0^2)\tan\left(\frac{\omega c_0}{2}\right) + c_0^2(1 - \nu^2), \quad \text{(A.33)}$$

$$B_8(\omega) = \omega(2U_0 - c_0^2)\cot(\omega c_0) + (1 + 2U_0\omega^2)c_0 - (2\nu^2 + \omega^2 c_0)c_0^2. \quad \text{(A.34)}$$

References

[1] M. Callegari, C.B. Carini, S. Lenci, E. Torselletti, L. Vitali, Dynamic models of marine pipelines for installation in deep and ultra-deep waters: analytical and numerical approaches, *Proceedings of AIMETA03*, Ferrara, 9–12 September 2003, CD-rom.

[2] L. Demeio, S. Lenci, Forced nonlinear oscillations of semi-infinite cables and beams resting on a unilateral elastic substrate, *Nonlinear Dynamics* 49 (2007) 203–215.

[3] G. Lancioni, S. Lenci, Forced nonlinear oscillations of a semi-infinite beam resting on a unilateral elastic soil: analytical and numerical solutions, *ASME Journal of Computational Nonlinear Dynamics* 2 (2007) 155–166.

[4] P.Y. Couliard, R.S. Langley, Nonlinear dynamics of deep-water moorings, *Proceedings of OMAE'01*, Rio de Janeiro, Brasil, 2001.

[5] J. Crank, *Free and Moving Boundary Problems*, Oxford University Press, Oxford, 1984.

[6] Y. Zhang, K.D. Murphy, Response of a finite beam in contact with a tensionless foundation under symmetric and asymmetric loading, *International Journal of Solids and Structures* 41 (2004) 6745–6758.

[7] J.-H. Yin, Comparative Modeling Study of Reinforced Beam on Elastic Foundation, *Journal of Geotechnical and Geoenviromental Engineering* 126 (2000) 265–271.

[8] N.C. Tsai, R.E. Westmann, Beams of tensionless foundation, *ASCE Journal of Engineering Mechanics* 93 (1967) 1–12.

[9] A.R.D. Silva, R.A.M. Silveira, R.A.M. Gonçalves, Numerical methods for analysis of plates on tensionless elastic foundations, *International Journal of Solids and Structures* 38 (2001) 2083–2100.

[10] D.M. Santee, P.B. Gonçalves, Oscillations of a beam on a non-linear elastic foundation under periodic loads, *Shock and Vibrations* 13 (2006) 273–284.

[11] O.R. Jaiswal, R.N. Iyengar, Dynamic response of a beam on elastic foundation of finite depth under a moving force, *Acta Mechanica* 96 (1993) 67–83.

[12] D.H.Y. Yen, C.T. Sing, On the non-linear response of an elastic string to a moving load, *International Journal of Non-Linear Mechanics* 5 (1970) 465–474.

[13] Y. Weitsman, On foundations that react in compression only, *ASME Journal of Applied Mechanics* 37 (1970) 1019–1030.

[14] Z. Celep, A. Malaika, M. Abu-Hussein, Forced vibrations of a beam on a tensionless foundation, *Journal of Sound and Vibration* 128 (1989) 235–246.

[15] I. Cokşun, The response of a finite beam on a tensionless Pasternak foundation subjected to a harmonic load, *European Journal of Mechanics A/Solids* 22 (2003) 151–161.

[16] I. Cokşun, Non-linear vibrations of a beam resting of a tensionless winkler foundation, *Journal of Sound and Vibration* 236 (2000) 401–411.

[17] R.F. Fung, C.C. Chen, Free and forced vibration of a cantilever beam contacting with a rigid cylindrical foundation, *Journal of Sound and Vibration* 202 (1997) 161–185.

[18] R. Toscano, Un problema dinamico per la piastra su suolo elastico unilaterale, in: G. Del Piero, F. Maceri (Eds.) *Unilateral Problems in Structural analysis, CISM Courses and Lectures no.* 288, 1985, pp. 375–387 (in Italian).

[19] J. Choros, G.G. Adams, A steadily moving load on an elastic beam resting on a tensionless Winkler foundation, *ASME Journal of Applied Mechanics* 46 (1979) 175–180.
[20] A.V. Metrikine, Steady state response of an infinite string on a non-linear visco-elastic foundation to moving point loads, *Journal of Sound and Vibration* 272 (2004) 1033–1046.
[21] G.G. Adams, An elastic strip pressed against an elastic half plane by a steadily moving force, *ASME Journal of Applied Mechanics* 45 (1978) 9–94.
[22] S. Lenci, M. Callegari, Simple analytical models for the J-lay problem, *Acta Mechanica* 178 (2005) 23–39.
[23] A. Nayfeh, *Perturbation Methods*, Wiley/Interscience, New York, 1973.
[24] A. Nayfeh, B. Balachandran, *Applied Nonlinear Dynamics*, Wiley/Interscience, New York, 1995.
[25] J.F. Doyle, *Wave Propagation in Structures*, Springer, Berlin, 1989.
[26] H. Kolsky, *Stress Waves in Solids*, Dover Publications, 1963.